Symmetry of Vibrationally Assisted Electronic Absorption and Emission Band Shapes of Impurities in Solids

C. Stuart Kelley*
Physical Research Division, Chemical Laboratory, Edgewood Arsenal, Aberdeen Proving Ground, Maryland 21010
(Received 18 January 1973)

For impurities that couple to the lattice through an interaction containing both linear and quadratic terms, mirror symmetry, at and above $T = 0$, of the resulting absorption and emission spectra about the zero-phonon line is highly dependent on the strength of the quadratic interaction parameter. Exact symmetry at all temperatures occurs only for the linear interaction. Overlap of the linear-plus-quadratic interaction spectra, although always in the vicinity of the zero-phonon line, is exactly coincident with the zero-phonon line at $T = 0$. Values of the linear and quadratic interaction parameters can be determined from the shapes of experimental broad-band spectra, the spacings of "hot lines," and the intensities of the zero-phonon lines.

I. INTRODUCTION

The vibrational interaction between an impurity ion and the host lattice in which it is embedded produces phonon-assisted transitions that accompany the purely electronic (zero-phonon) transitions within the impurity. The most widely used approximation to this interaction has been the linear interaction,[1] wherein the vibrational frequencies of the ground and excited states are equal. The semiclassical approximation,[2,3] which treats the initial state quantum mechanically and the final state classically, has been successful in fitting broad unstructured absorption and emission bands. The quantum-mechanical treatment[1,4,5] of the linear interaction illustrates the vibronic structure that occurs on the zero-phonon sides of the bands found in many impurity-related spectra. This vibronic structure contains a wealth of information concerning the nature of the vibronic interaction.

The linear interaction produces an emission spectrum that is the mirror image of the absorption spectrum, as rotated about the zero-phonon line; their intersection coincides with the zero-phonon line. This mirror symmetry thus provides, especially for T well above $T = 0$, a means for identifying zero-phonon lines from phonon-assisted lines.

For an impurity at a site of inversion symmetry, the quadratic-vibrational-interaction term can be important for certain modes of vibration.[6,7] The symmetry of absorption and emission spectra that result is treated in detail elsewhere.[8] In essence, the spectra show near-mirror symmetry for T near zero, but are virtually identical at higher temperatures.

Using the convolution approach of Ritter[5] to the linear interaction, Mostoller *et al.*[9] successfully fitted the $T = 0$ absorption spectrum of the N_1 color center in NaCl. The quadratic interaction was included to first order in their prediction of the $T = 0$ emission spectrum. Effects of the quadratic interaction on the band shape have been reported,[10,11] and have been included in comparisons of the theory with experimental results.[11,12]

In the present paper, the concern is the extent to which mirror symmetry occurs between the $T > 0$ absorption and emission band shapes that result from the general interaction. The basic complication is that the absorption and emission band shapes due to a single vibrational mode are dependent on three parameters: the linear interaction parameter (or Huang-Rhys factor), the quadratic interaction parameter, and the temperature. The procedure is to review the theory of band shapes, present representative examples of absorption and emission spectra at and above $T = 0$, compare these band shapes to those in the limiting cases of the linear and quadratic interactions, and provide methods for estimating the values of the linear and quadratic interaction parameters from experimental spectra.

II. THEORETICAL BAND SHAPES

The complete quantum-mechanical derivation of the absorption and emission band shapes was presented earlier.[6] Basically, the absorption or emission intensity I as a function of energy E and temperature T is the sum over the initial and final vibrational levels of the product of the square of the matrix element for the electric dipole transition and the thermal population factor. For absorption,

$$I_\alpha(E, T) = \sum_{i,f} \langle \Psi_{ai} | e\vec{r} | \Psi_{bf} \rangle^2 B_{ai}\, \delta(E - E_{bf} + E_{ai}). \quad (1)$$

The subscripts a and b denote the ground and excited electronic states and Ψ are the wave functions for these states. The thermal population factor for the ith vibrational level of the ground state is B_{ai}, and the δ function locates the energy of the

$i \rightarrow f$ transition. Applying the adiabatic and Born-Oppenheimer approximations, we have

$$\langle \Psi_{ai} | e\vec{r} | \Psi_{bf} \rangle = \langle \phi_a | e\vec{r} | \phi_b \rangle \langle \chi_{ai} | \chi_{bf} \rangle \ ,$$

where ϕ are the purely electronic wave functions and the χ are the purely vibrational wave functions. The ground- and excited-state potential energies for the vibrational motion are parabolic in the normal coordinate that specifies the interaction between the impurity ion and the lattice. The minima of the ground- and excited-state potential energy curves are separated by the energy E_0 and the normal coordinate q_0. The excited state is characterized by a vibrational frequency ω_b that is a factor of R (the quadratic interaction parameter, which is related to a similar measure D of the quadratic interaction used by Pekarek and Markham[13] by $R = D + 1$) times that of the ground state ω_a. Defining $\Theta = \hbar\omega_a/k$ and the Huang-Rhys factor $S = \omega_a q_0^2/2\hbar$, the band shapes for absorption and emission become

$$I_\alpha(E, T) = K_\alpha C_{ab}^2 (1 - e^{-\Theta/T}) \sum_{i,f} \langle \chi_{ai} | \chi_{bf} \rangle^2 e^{-i\Theta/T} \times \delta\{E - E_0 - \tfrac{1}{2}[R(1-2S) - 1]\hbar\omega_a - (Rf - i)\hbar\omega_a\} \quad (2)$$

and

$$I_\epsilon(E, T) = K_\epsilon C_{ba}^2 (1 - e^{-R\Theta/T}) \sum_{i,f} \langle \chi_{bf} | \chi_{ai} \rangle^2 e^{-fR\Theta/T} \times \delta\{E - E_0 - \tfrac{1}{2}[R(1-2S) - 1]\hbar\omega_a - (Rf - i)\hbar\omega_a\} , \quad (3)$$

where $C_{ab} = \langle \phi_a | e\vec{r} | \phi_b \rangle$ and $C_{ba} = \langle \phi_b | e\vec{r} | \phi_a \rangle$. As

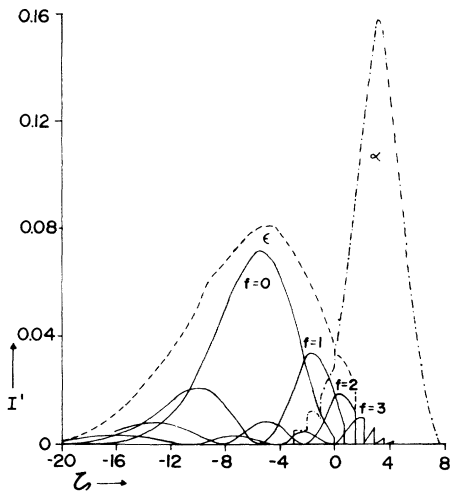

FIG. 1. I' (proportional to absorption and emission intensity) vs ζ (proportional to photon energy) at $T = \Theta$ for $R = 0.72$ and $S = 4.5$. The dashed line is the over-all emission band shape. Contributions to the over-all band shape for the $f = 0$, 1, 2, and 3 envelopes are shown by the solid lines. The dot-dash line is the absorption band shape.

is customary, K_α, C_{ab}, and C_{ba} are considered to be constants. It is further assumed, for convenience, that K_ϵ is constant, although it does, in fact, have an E^3 dependence.[2] Also, any Jahn-Teller effects are ignored. The matrix element has been available for some time.[14] It may be written

$$\langle \chi_{ai} | \chi_{bf} \rangle = (-1)^f \left(\frac{2^{i+f+1} R^{i+1/2} i! f!}{1+R}\right)^{1/2} \times \left(\frac{(2S)^{1/2}}{1+R}\right)^{i+f} e^{-S/(1+R)} \times \sum_{l=0} \left(\frac{1+R}{-2S}\right)^l (l!)^{-1} \sum_{j=0} \left(\frac{1-R^2}{8SR}\right)^j [j!(i-l-2j)!]^{-1} \times \sum_{m=0} \left(\frac{1-R^2}{-8S}\right)^m [m!(f-l-2m)!]^{-1} \ . \quad (4)$$

The general interaction occurs for $R \neq 1$ and $S \neq 0$, whereas the linear interaction is characterized by $R = 1$, and the quadratic interaction by $S = 0$.

III. CALCULATIONS AND DISCUSSION

Representative absorption and emission spectra were calculated from Eqs. (2) and (3) using the matrix elements given by Eq. (4). The calculations included contributions from i, $f \leq 26$, which amply illustrate the features of the spectra. The computer print-out consisted of a series of spikes for each value of i in absorption and f in emission, any one series having a smooth envelope. As in previous papers,[6,8] these envelopes were summed to give the over-all absorption and emission band shapes. This method of construction of the band shape is shown in Fig. 1. The ordinate of each of the figures is $I'(E, T) = IK^{-1}C^{-2}$, which is proportional to the absorption or emission intensity. Each abscissa is $\zeta = Rf - i$ and is proportional to the photon energy. The values of R, S, and T/Θ characterize each spectrum. Values of $T/\Theta = 0$, 1, and 3 correspond very roughly to liquid-helium, liquid-nitrogen, and room temperatures, if $\Theta = 100$ K, although actual values of Θ can vary appreciably.

Typical absorption and emission spectra resulting from the linear interaction ($R = 1$) are shown in Fig. 2. For all temperatures, the spectra are exact mirror images as rotated about the zero-phonon line. If normalized to the same peak intensity, experimental absorption and emission spectra from such a system will have equal half-widths, and will always overlap at the zero-phonon line. The $T = 0$ spectra peak at $i, f \simeq S - \frac{1}{2}$. The broadening of the absorption and emission bands with increasing temperature is nearly symmetric on both sides of their respective peaks, and the peaks are still located at $i, f \simeq S - \frac{1}{2}$. For large values of the Huang-Rhys factor ($S \gtrsim 20$, say), the absorption and emission bands are smooth and

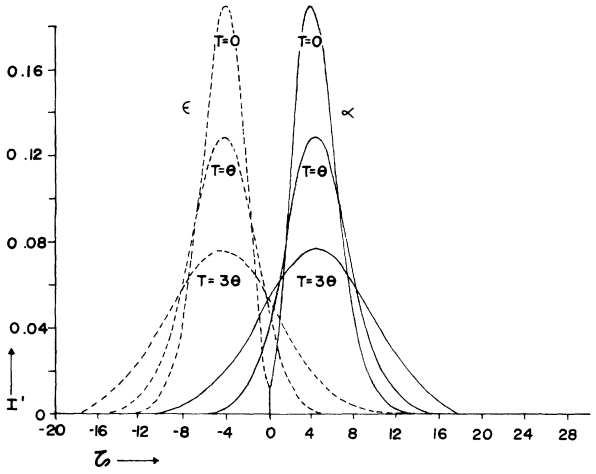

FIG. 2. I' (proportional to absorption and emission intensity) vs ζ (proportional to photon energy) at $T=0$, Θ, and 3Θ for the linear interaction, $R=1$, with $S=4.5$. The dashed lines are the over-all emission band shapes, and the solid lines are the over-all absorption band shapes. There is exact mirror symmetry of the spectra about the common zero-phonon line.

Gaussian shaped and thereby well described by the semiclassical approximation,[1] which is not applicable to structured and asymmetric band shapes. The symmetry and shape of the spectra that result from the quadratic interaction are described briefly in Sec. I and in a previous paper.[8]

For systems having both linear and quadratic interaction terms, mirror symmetry of the spectra is broken. The absorption and emission spectra have different peak intensities, peak energies, and half-widths. At $T=0$, the spectra always overlap at the zero-phonon line that is the low-energy cutoff for absorption and the high-energy cutoff for emission [see Fig. 3(a), for example].

Experimental absorption and emission spectra may be normalized by equating their intensities at the zero-phonon line cutoff. With this normalization, the peak intensity for emission is less than that for absorption if $R<1$, and greater for $R>1$ [Figs. 3(a), 4(a), 5(a), and 6(a)]. The separation in energy of the peak of the band and the zero-phonon line for emission is greater than that for absorption if $R<1$, and less if $R>1$. The half-width for emission is greater than that for absorption if $R<1$, and less if $R>1$. This method presupposes the identification of the zero-phonon line, and accordingly may have limited application.

The value of R is roughly given by $\zeta_{a_{\text{peak}}}/\zeta_{\epsilon_{\text{peak}}} \simeq -R$ (see below) and $I_{\epsilon_{\text{peak}}}/I_{a_{\text{peak}}} \simeq R$. With increasing R (Figs. 2, 5, and 6) the peaks of both the absorption and emission bands shift to higher energy. With increasing S (Figs. 1, 3, and 4), the peak of the absorption band shifts to higher energy, while the peak of the emission band shifts to lower energy. As shown earlier,[6] the $T=0$ absorption band peaks near

$$\zeta_{a_{\text{peak}}} = [4SR/(1+R)^2] \exp[-2(1-R)/(1+R)],$$

which, for $R=1$, reduces to S, the usual linear interaction result.[10] The $T=0$ emission band peaks near

$$\zeta_{\epsilon_{\text{peak}}} = [-4S/(1+R)^2] \exp[-2(1-R)/(1+R)],$$

so that $R\zeta_{\epsilon_{\text{peak}}} \simeq -\zeta_{a_{\text{peak}}}$.

From the $T=0$ absorption spectrum, the ratio of the intensity of the one-phonon-assisted line to the intensity of the zero-phonon line $I_{a_1}/I_{a_0} = 4S/(1+R)^2$ can be used to estimate the value of the Huang-Rhys factor provided the value of R is known.

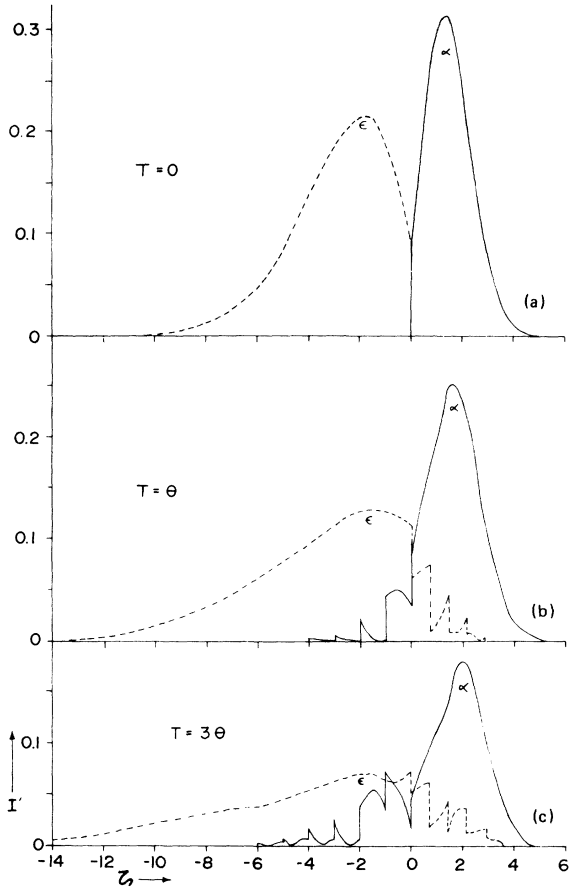

FIG. 3. I' (proportional to absorption and emission intensity) vs ζ (proportional to photon energy) for $R=0.72$ and $S=2.0$: (a) at $T=0$, (b) at $T=\Theta$, and (c) at $T=3\Theta$. The solid line is the absorption band and the dashed line is the emission band. Because $R<1$, the peak absorption intensity is greater than the peak emission intensity, the absorption half-width is less than that for emission, and the separation of the absorption peak from the zero-phonon line is less than that for emission. The opposite holds for $R>1$ (see Fig. 5).

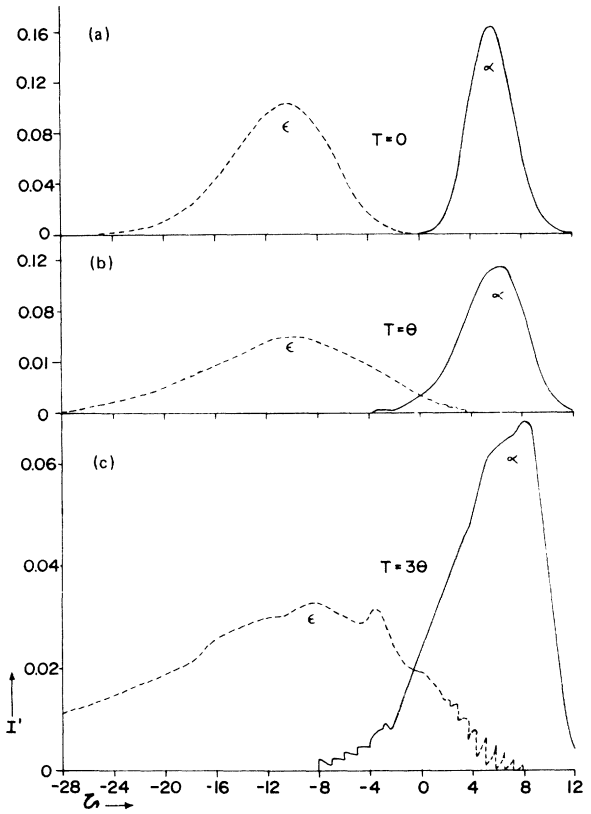

FIG. 4. I' (proportional to absorption and emission intensity) vs ζ (proportional to photon energy) for $R=0.72$ and $S=8$: (a) at $T=0$, (b) at $T=\Theta$, and (c) at $T=3\Theta$. The solid line is the absorption band; the dashed line is the emission band. The intersection of the spectra for $T>0$ is not necessarily coincident with the zero-phonon line. The spacings of the absorption and emission "hot lines" can be used to determine precisely the value of R.

For emission,

$$I_{\epsilon_1}/I_{\epsilon_0}=4SR/(1+R)^2.$$

In fact, the required value of R can be found exactly from the ratio of these two ratios, or $I_{\epsilon_1}/I_{a_1}=R$.

The shape of the $T=0$ spectrum persists, with modifications, to higher temperatures. Because the dominant transitions in absorption and emission are from $i=0$ and $f=0$, respectively, the peaks of the over-all band shapes occur roughly as they do at $T=0$ (Fig. 1), and the statements above concerning the breadths, peak intensities, and energies of the peaks are applicable generally for $T>0$. Due to contributions from $i>0$ in absorption and $f>0$ in emission, the $T>0$ spectra no longer intersect rigorously at the zero-phonon line [see Fig. 4(c)]; however, their intersection remains close to the zero-phonon line.

As T increases, the zero-phonon side of each spectrum develops structure (so-called "hot lines"), while the other side of the band retains its smooth nature. Each band broadens and decreases in peak intensity. Broadening occurs predominantly on the zero-phonon side of the band. The hot lines in emission, originating from the population of levels other than $f=0$, are shown in Fig. 1. The peak at the highest energy for each f envelope is primarily responsible for each of these hot lines. A similar situation occurs in absorption, and provides a precise means for determining R. The energy difference between adjacent hot lines in emission is just R times that for absorption, $\Delta\zeta_{\text{hot}_\epsilon}/\Delta\zeta_{\text{hot}_a}=R$. For example, from Fig. 1,

$$[2.88-2.16]/[-2-(-3)]=0.72.$$

The intensity of the $T=0$ zero-phonon line is $[2\sqrt{R}/(1+R)]\exp[-2S/(1+R)]$. For $4S^2\gg 1$ (typically, $S>2$, although, in fact, S can vary from 0 to 100), the intensity of the zero-phonon line in-

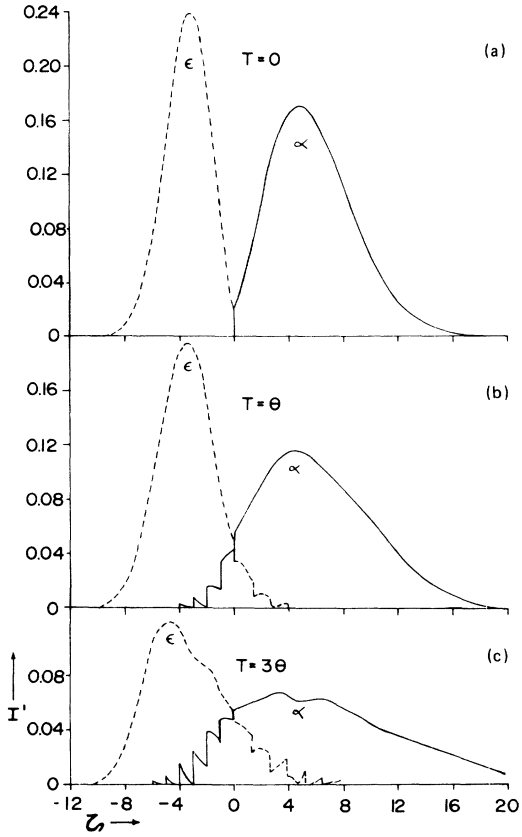

FIG. 5. I' (proportional to absorption and emission intensity) vs ζ (proportional to photon energy) for $R=1.3$ and $S=4.5$: (a) at $T=0$, (b) at $T=\Theta$, and (c) at $T=3\Theta$. The solid line is the absorption band; the dashed line is the emission band. The ratios of absorption to emission peak intensities, half-widths, and separations of peaks from the zero-phonon lines are reversed from those when $R<1$ (see Fig. 3).

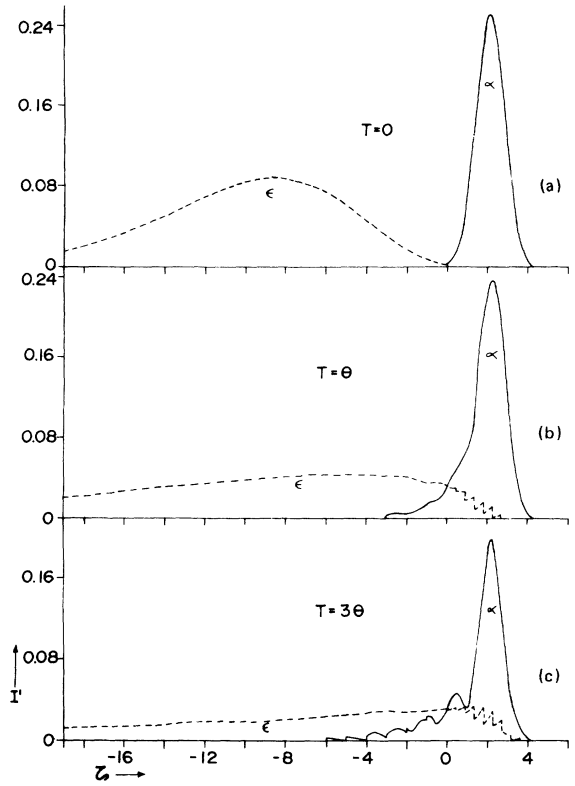

FIG. 6. I' (proportional to absorption and emission intensity) vs ζ (proportional to photon energy) for $R=0.45$ and $S=4.5$: (a) at $T=0$, (b) at $T=\Theta$, and (c) at $T=3\Theta$. The solid line is the absorption band; the dashed line is the emission band. The intensities of the zero-phonon lines decrease exponentially with S.

creases smoothly with increasing R [Figs. 6(a), 2, and 5(a)]. Thus, the strongly quadratic zero-phonon line ($R \neq 1$, with $R > 1$) is more intense than the weakly quadratic zero-phonon line ($R \simeq 1$). Once R is known, the value of S can be determined from the $T=0$ zero-phonon line intensity. For any given impurity system, the zero-phonon lines in absorption and emission are identical for $T=0$. At higher temperatures, they are still nearly identical for $R \simeq 1$.

In emission, as in absorption,[6] the value of the Huang-Rhys factor can be estimated from the intensity of the experimentally observed zero-phonon line; at $T=0$, the zero-phonon line intensity decreases with S as $\exp[-2S/(1+R)]$. Thus, the zero-phonon line is not easily observed in systems having a strong linear interaction as, for example, in systems describable by the semiclassical approximation.

IV. CONCLUSIONS

The general impurity-lattice vibrational interaction, containing both linear and quadratic terms, has only recently been applied to predict absorption spectra at temperatures other than $T=0$, and not at all to emission spectra. Specific examples of such absorption and emission spectra are presented here, and compared to spectra from the limiting cases of the linear interaction and the quadratic interaction. The strength of the quadratic interaction parameter is shown to determine the degree of mirror asymmetry of the spectra about the zero-phonon line. Exact mirror symmetry occurs only for the linear interaction. Although the absorption and emission spectra always overlap at the zero-phonon line for $T=0$, the general interaction spectra at $T>0$ do not necessarily overlap at the zero-phonon line. The intersection of the spectra, however, remains close to the zero-phonon line. From experimental absorption and emission spectra the value of the quadratic interaction parameter can be determined from the shapes of the $T=0$ bands, the intensities of the zero- and first-phonon lines at $T=0$, and the spacings of the hot lines at $T>0$. Once the quadratic interaction parameter is known, the Huang-Rhys factor can be determined from the energies of the peaks of the $T=0$ bands, or from the intensity of the zero-phonon line at $T=0$.

ACKNOWLEDGMENT

The author is appreciative to T. W. Crimmins for preparing the computer program used to compute the line intensities.

*Present address: General Research Corp., 1501 Wilson Blvd., Arlington, Va. 22209.

[1]T. H. Keil, Phys. Rev. **140**, A601 (1965).
[2]M. Lax, J. Chem. Phys. **20**, 1752 (1952).
[3]F. E. Williams and M. H. Hebb, Phys. Rev. **84**, 1181 (1951).
[4]J. T. Ritter and J. J. Markham, Phys. Rev. **185**, 1201 (1969).
[5]J. T. Ritter, J. Chem. Phys. **53**, 3461 (1970).
[6]C. S. Kelley, Phys. Rev. B **6**, 4112 (1972).
[7]C. H. Henry, S. E. Schnatterly, and C. P. Slichter, Phys. Rev. **137**, A583 (1965).
[8]C. S. Kelley, Phys. Rev. B **6**, 4763 (1972).
[9]M. Mostoller, B. N. Ganguly, and R. F. Wood, Phys. Rev. B **4**, 2015 (1971).
[10]J. J. Markham, Rev. Mod. Phys. **31**, 956 (1959).
[11]P. W. M. Jacobs and A. K. Menon, J. Chem. Phys. **55**, 5357 (1971).
[12]J. D. Konitzer and J. J. Markham, J. Chem. Phys. **32**, 843 (1960).
[13]N. Z. Pekarek and J. J. Markham, Phys. Lett. A **38**, 505 (1972).
[14]E. Hutchisson, Phys. Rev. **36**, 410 (1930); Phys. Rev. **37**, 45 (1931).